Three-dimensional free surface modelling in an unstructured mesh environment for metal processing applications.

K. A. Pericleous, G. J. Moran, S. M. Bounds, P. Chow*and M. Cross
Centre for Numerical Modelling and Process Analysis,
University of Greenwich,
London SE18 6PF, UK
e-mail : K. Pericleous@gre.ac.uk

ABSTRACT

In the casting of metals, tundish flow, welding, converters, and other metal processing applications, the behaviour of the fluid surface is important. In aluminium alloys, for example, oxides formed on the surface may be drawn into the body of the melt where they act as faults in the solidified product affecting cast quality. For this reason, accurate description of wave behaviour, air entrapment, and other effects need to be modelled, in the presence of heat transfer and possibly phase change. The authors have developed a single-phase algorithm for modelling this problem. SEA or the Scalar Equation Algorithm (see Chan et al.[1],Pericleous et al. [2]), enables the transport of the property discontinuity representing the free surface through a fixed grid. An extension of this method to unstructured mesh codes is presented here, together with validation. The new method employs a TVD limiter in conjunction with a ray-tracing algorithm, to ensure a sharp bound interface. Applications of the method are in the filling and emptying of mould cavities, with heat transfer and phase change.

1 INTRODUCTION

Metal casting is one of the oldest technologies in the world and yet it is still used in the manufacture of some of the highest integrity components in the aerospace, automotive and other high-tec industries. Though better controlled and more sophisticated in its technological context, the casting process is essentially the same as it ever was - hot liquid metal is poured into a mould and then solidifies[3]. This simple statement belies the fact that the above process involves a range of interacting physical phenomena, including:

- free surface fluid flow as the mould fills,
- convection once the mould has filled,
- heat transfer from the metal to the mould,
- solidification of the metal as it cools.

This multi-phase problem can be solved efficiently using a single-phase scalar marker technique. The authors, building on the work of Jun and Spalding[4], have demonstrated that heat transfer[1], and simultaneous change of phase[2] can be accommodated within a fixed mesh computational domain, containing a dynamically varying discontinuity interface. Great care needs to be taken in the numerical scheme used, to prevent numerical smearing at the interface. The TVD scheme of van Leer[5] was found to be particularly attractive in this context. The resulting SEA[1](Scalar Equation Algorithm) method, although similar in concept to the popular VoF method of Hirt and

*Present address: Fujitsu UK.

Nichols[6], differs in that the solution covers both the gas and the liquid regions of the domain. This is important in casting, as it enables proper account of the mixing of gas and liquid to be considered. Such mixing is undesirable in castings, and indeed a commonplace feature in poorly designed running systems[7].

The present contribution extends the SEA method to accommodate unstructured meshes. This facility is necessary for filling simulations of castings, where not only the mould, but also the complete running system has to be meshed. The adoption of an unstructured mesh is also desirable, since post-fill, or even concurrent stress-strain computations are required in the solidified portion of the metal to compute distortion[8] – the stress computations usually require FE type unstructured mesh topolgy. The van Leer scheme was generalised for this purpose using a ray-tracing technique in the flow direction, so that the most 'appropriate' value of the upstream variable is used in the flux limiter.

The paper contains a mathematical description of the problem considered, numerical schemes used, and a brief outline of the solution procedure within the Unstructured-Mesh-Finite-Volume code PHYSICA[9]. This is followed by example applications, which include validation. Suggestions for future research are contained in the concluding section.

2 MATHEMATICAL DESCRIPTION

2.1 The Fluid flow equation.

The general equations that govern three-dimensional transient fluid flow are given by the momentum and mass continuity equations which are stated in their vector form below,

$$\frac{\partial}{\partial t}(\rho \underline{u}) + \nabla.(\rho \underline{u}\underline{u}) = \nabla.(\mu \nabla \underline{u}) - \nabla p + \underline{S} \quad (1)$$

$$\frac{\partial \rho}{\partial t} + \nabla.(\rho \underline{u}) = 0 \quad (2)$$

where $\underline{u}$ is the velocity vector. The other variables at time t are ρ, the material density, μ, the dynamic viscosity, and the pressure p. The vector source term $\underline{S}$ in equation(1) represents body forces, and the influence of boundaries.

For solidification problems, the source term $\underline{S}$ in equation(1) represents a flow resistance provided by the solid phase, see reference [8].

2.2 The Free Surface model.

For incompressible flows, the mass continuity equation(2) can be rewritten as

$$\nabla.\underline{u} = 0 \quad (3)$$

This equation forms the basis of the GALA algorithm originally developed by Spalding[10] for flows with large changes in density.

The Scalar Equation Algorithm (SEA) method has been used successfully in casting simulations with structured meshes[1, 2]. The method employs a scalar Φ to represent the metal volume fraction in a control volume cell. In a gas cell, $\Phi = 0$, in a metal cell, $\Phi = 1$, and Φ takes on an intermediate value for a partially filled cell.

The momentum equation (1) is rewritten as

$$\frac{\partial}{\partial t}(\rho_{gas} \underline{u}) + \nabla.(\rho_{gas} \underline{u}\underline{u}) = \nabla.(\mu \nabla \underline{u}) - r \nabla p + \underline{S} \quad (4)$$

the factor r in the pressure gradient term, is given by

$$r = \left\{ 1 + \Phi \left(\frac{\rho_m}{\rho_{gas}} - 1 \right) \right\}^{-1} \quad (5)$$

where ρ_{gas} and ρ_m are the gas and metal density respectively. Hence, when $\Phi = 0$, the momentum equations will use the gas density and when $\Phi = 1$, the metal density will be used. The mixture density and

viscosity are based on the value of Φ. The viscosity is given by

$$\mu = \mu_{gas} + \Phi\left[\left(\mu_m \frac{\rho_{gas}}{\rho_m}\right) - \mu_{gas}\right] \quad (6)$$

and the mixture density is

$$\rho = \rho_{gas} + \Phi(\rho_m - \rho_{gas}) \quad (7)$$

Further details can be found in reference[11].

2.3 Free Surface Dynamics.

The dynamics of the free surface are governed by the motion of Φ which obeys the advection equation,

$$\frac{\partial \Phi}{\partial t} + \nabla.(\Phi \underline{u}) = 0 \quad (8)$$

On the assumption that the motion of Φ is governed solely by convection. Equation(8) integrated over the control volume gives,

$$\int_t \int_V \frac{\partial \Phi}{\partial t} dV dt + \int_s \Phi \underline{u} ds_i = 0 \quad (9)$$

In discrete form of this equation gives,

$$\Phi_p^{n+1} = \Phi_p^n - \sum_{i=1}^{Faces} \frac{\underline{u}_i^{n+1}.\underline{n}_i A_i \Delta t}{V_p} \Phi_{i(U)}^n \quad (10)$$

where the subscript i sums over the faces of the control volume P. The second term on the RHS of equation(10) is the flux summation term. The value $\Phi_{i(U)}$ is the value of Φ at the face, which, in this study, is taken to be the upwind cell value denoted by the subscript U (D will refer to the cell that shares face i, as shown in Figure(1)). The velocity $\underline{u}_i^{n+1}$ is the latest value of the face velocity and $\underline{n}$ is the surface normal of face i.

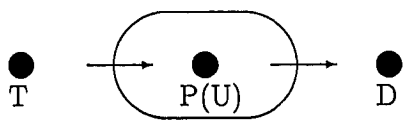

Figure 1: Definition of the cell positions.

The term $\underline{u}_i^{n+1}.\underline{n}_i A_i \Delta t V_p^{-1}$ in the flux summation term of equation (10), is the Courant-Friedrichs-Lewy(CFL) stability number,

$$\sigma_i = \frac{\underline{u}_i^{n+1}.\underline{n}_i A_i \Delta t}{V_p} \quad (11)$$

therefore, equation (10) can be rewritten in terms of σ_i,

$$\Phi_p^{n+1} = \Phi_p^n - \sum_{i=1}^{Faces} \sigma_i \Phi_U^n \quad (12)$$

For stable solutions of this explicit equation, the value of σ_i must always be in the range $|\sigma_i| \leq \frac{1}{\sqrt{N}}$ where N is the number of spatial dimensions. In equation(11), σ_i is a three dimensional quantity; however similar expressions can be defined for σ_i for one and two dimensions.

When first order differencing schemes (hybrid, upwind, etc.) are used to solve the advection equation(12), the interface is found to smear out. Various techniques can be used to combat this numerical smearing. In this study, the van Leer[5] TVD scheme is adopted, as being the simplest to implement and most economical of the higher order schemes available[12].

The algebraic description of van Leer's algorithm is

$$\Phi_U^n = \Phi_U^n + (1 - \sigma_i)\overline{\Delta_p}\Phi \quad (13)$$

where

$$\overline{\Delta_p}\Phi = \begin{cases} \delta sgn(\Delta^+) & \text{if} \Delta^+.\Delta^- \leq 0 \\ 0 & \text{otherwise} \end{cases} \quad (14)$$

with

$$\begin{aligned} \Delta^+ &= \Phi_D - \Phi_P \\ \Delta^- &= \Phi_P - \Phi_T \end{aligned} \quad (15)$$

and

$$\delta = min(|\Delta^+|, |\Delta^-|, \frac{1}{2}|\Phi_D - \Phi_T|) \quad (16)$$

Equation(10) is used in conjunction with the converged face velocities and TVD correction (equation(13)) to update the scalar field Φ. The TVD flux limiter is applied

along the flow direction. As the flow may change direction many times during a simulation, an adaptive limiter is used, in which a ray tracing algorithm is used along the direction of the flow to detect the most suitable cell value(cell T in Figure(1)). In a multi-dimensional problem, as shown in Figure(2), material flows from cell β to cell α. If the face velocity is $v1$, then the value of Φ in cell γ is used in the TVD limiter. For a face velocity, $v2$, the value of cell δ is used.

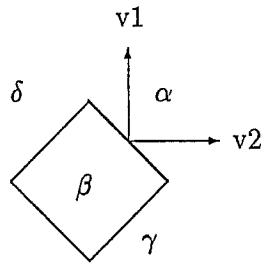

Figure 2: Application of the ray tracing algorithm.

2.4 Heat Transfer and Solidification.

Transient heat flow is described by the energy equation(17),

$$\frac{\partial}{\partial t}(\rho h) + \nabla.(\rho h \underline{u}) = \nabla.(\Gamma \nabla h) + S^h \quad (17)$$

Written in this form, the exchange coefficient Γ represents the ratio of conductivity over specific heat in the fluid, that is, $\Gamma = k/C_p$. The source term S^h represents viscous dissipation, heat entering the domain due to fluid bulk motion, heat transfer at the walls, and in this study change of phase. The source term S^h, takes account of the evolution of the latent heat L during solidification, and is defined as

$$S^h = -\frac{\partial}{\partial t}(\Phi \rho_m f_L L) - \nabla.(\Phi \rho_m \underline{u} f_L L) \quad (18)$$

where f_L is the liquid fraction of the metal component of the fluid. Typically, the liquid fraction is a function of the metal temperature; one simple and popular relationship is

$$f_L = \begin{cases} 1 & T > T_L, \text{ the liquidus temp} \\ \left(\frac{T-T_S}{T_L-T_S}\right) & T_S \leq T \leq T_L, \text{in the mushy zone} \\ 0 & T < T_S, \text{the solidus temp} \end{cases} \quad (19)$$

The presence of metal at any location is determined by the scalar Φ, which allows one to define gas-metal properties, see equations(6 & 7).

2.5 Overall Solution Procedure.

The solution procedure is based upon the iterative SIMPLE algorithm of Patankar and Spalding[13], which is the standard FV scheme for engineering fluid flows. It is enhanced in various ways to reflect the additional computational difficulties associated with free surface problems involving simultaneous heat transfer and solidification. The procedure to advance the solution from time t^n to t^{n+1} comprises the following steps:

1. Begin with initial variable fields, $\underline{u}^n$, Φ^n, h^n, f_L^n and material properties ρ^n, μ^n, k^n, C_p^n .
2. Solve the momentum equations (1) using a guessed pressure field.
3. Compute the volume continuity errors and form a pressure correction equation from equation(3).
4. Apply velocity corrections (to obtain $\underline{u}^{n+1}$) and pressure corrections to reduce continuity errors.
5. Solve energy equation(17) to obtain h^{n+1} and determine the latest temperature T^{n+1}.
6. Update the scalar field Φ^{n+1} using $\underline{u}^{n+1}$ and the van Leer corrections.

7. Calculate f_l^{n+1} from T^{n+1} and determine heat released during solidification.

8. Update material properties ρ^{n+1}, μ^{n+1}, k^{n+1}, C_p^{n+1}.

9. Repeat steps 2-8 until errors in solution variables have fallen below predetermined limits.

In solving equation(17), material properties at time t^{n+1} are employed within the iterative loop in order to conserve energy. For example, the temporally discretised form of equation (18) is

$$S^h = \rho_m L \left[\frac{\Phi^n f_L^n}{\Delta t} - \frac{\Phi^{n+1} f_L^{n+1}}{\Delta t} - \nabla.(\Phi^n \underline{u}^{n+1} f_L^n) \right] \quad (20)$$

When spatially discretised, the product $\Phi^n \underline{u}^{n+1}$ is replaced by fluxes provided by the van Leer scheme which ensures compatibility with equation (12). This procedure applies to the advection of any material property dependent on Φ and avoids the significant errors that might otherwise result from the large and abrupt changes in properties at the gas-metal interface. Fluid flow material properties are always based on Φ^n in order to avoid numerical instabilities.

3 RESULTS

3.1 Issues of Validation.

At the time of writing, there were no benchmark sets of experimental results for the validation of free surface problems with simultaneous heat transfer/solidification. However, there are a number of benchmarks for free surface flows, and a good analytic solution test case for the simultaneous fluid flow and heat transfer with solidification.

The first case is based on an experiment of a collapsing water column, performed by Martin and Moyce[15] published in 1952. The water column is initially in hydrostatic equilibrium before the right wall is instantly removed and the water column collapses under gravitational acceleration (see Figure 2 for the set-up and an example of the results). Figure (4) shows the numerical prediction for the height position as a function of time compared to experimental data. The agreement is very good, given the approximations inherent in the model (e.g no explicit representation of turbulence). The calculations were carried out with the PHYSICA[9] code, using a variety of meshes up to 3960 cells (99x40) in size.

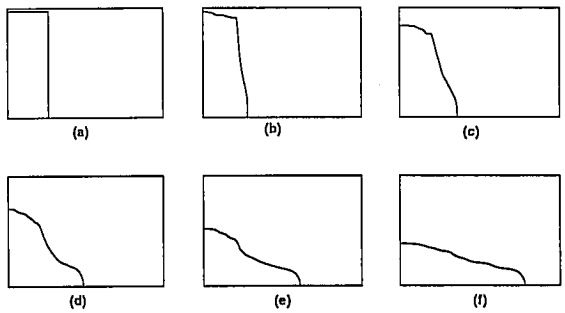

Figure 3: Collapsing column, profiles of Φ = 0.5 as time advances.

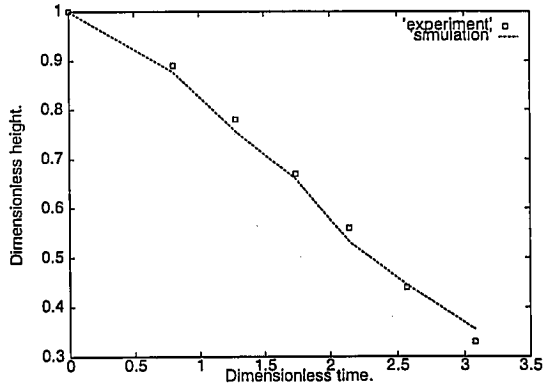

Figure 4: Collapsing water column, height vs time.

The next testcase involves a pipe, initially full with air, being filled with water flowing at a constant rate. The problem was modelled using the deliberately complex unstructed mesh shown in Figure(5). Inlet and outlet boundary conditions were imposed, which are labelled I and O respectively in

Figure(5) and water allowed to enter the pipe through the inlet. The material properties are shown in Table(3) and boundary conditions shown in Table(1). The direction of flow is also shown in Figure(5). The free surface was then monitored during its passage along the plane, and remained well defined during its passage, in spite of the mesh complexity, as shown in Figures (6 & 7). On average, the front was found to be smeared over four cells in the direction of propagation. The position of the free surface can be compared with the predicted signal propagation speed $\underline{u}\Delta t$ and the agreement is very good.

The next case tests the coupling between the free surface, heat transfer, solidification and fluid flow equations. A cavity (see Figure 8 for the mesh), initially containing gas at $10°C$, is filled with liquid, also at $10°C$. During the filling the liquid cools and solidifies.

The boundary conditions and material properties are shown in Tables (2 & 3). The solidus and liquidus temperatures are $5°C$ and $6°C$ respectively, and the latent heat is 50 kJ/kg. Solid material was allowed to move in the flow.

The boundary conditions and low gas conductivity render heat transfer in the liquid/solid approximately one-dimensional in y. Therefore, it is possible to compare the temperature predictions against a reference solution obtained from the numerical solution of a one-dimensional heat transfer/solidification problem. Figure 9 shows the temperature histories of points positioned at A(5, 5), B(10, 5) and C(15, 5) within the cavity, which should predict the gas temperature for times up to 2, 4 and 6 seconds respectively, and the metal temperature thereafter. The plots indicate that due to the finite gas conductivity and low thermal capacitance, the gas temperature decreases ahead of the free surface. However, this conduction does not represent a significant transfer of heat and the temperature predictions within the liquid/solid compare well with those given by the reference solution.

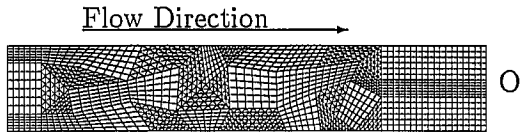

Figure 5: Two-dimensional unstructured mesh for validation case 2.

Figure 6: Mid way position of the free surface (white/black represents metal/gas).

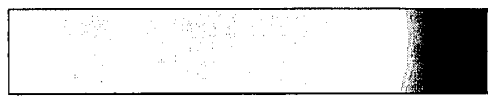

Figure 7: Final position of the free surface (white/black represents metal/gas).

Table 1: Boundary conditions for case 2

$x = 0m$	$u_x = 1m/s$
$x = 5m$	$P = 0\ N/m^2$
$y = 0m$	$\partial u_x/\partial y = 0$
$y = 1m$	$\partial u_x/\partial y = 0$

Table 2: Boundary conditions for case 3

$x = 0mm$	$u_x = 2.5mm/s$	$\partial T/\partial x = 0$
$x = 20mm$	$P = 0\ N/m^2$	$\partial T/\partial x = 0$
$y = 0mm$	$\partial u_x/\partial y = 0$	$\partial T/\partial y = 0$
$y = 10mm$	$\partial u_x/\partial y = 0$	$T = 0°C$

Table 3: Material Properties for cases 2 & 3

Gas Properties	Liquid Properties
$\rho = 1kg/m^3$	$\rho = 1000kg/m^3$
$k = 0.01W/m°C$	$k = 100W/m°C$
$C_p = 1kJ/kg°C$	$C_p = 1kJ/kg°C$
$\mu = 1 \times 10^{-5}kg/ms$	$\mu = 0.01kg/ms$

The final case was that of mould filling with an attached running system. In this case a square cavity is filled, but the feeder, sprue, runners and gates are also included in the simulation. The mesh contains 10,000 elements with inlet/outlet boundary conditions on the top of the sprue/feeder respectively. One can see from the sequence of pictures shown in Figure(10), that complex wave behaviour occurs during filling. In Figure (10a), liquid can be seen entering the cavity through the running system. Liquid from both gates meets and interacts, forming surface waves, as seen in Figure (10b). These waves persist even when the cavity is full and the feeder is filling, see (10c), until the the mould fills as shown in Figure (10d). The results enclosed were produced on a SUN Sparc Ultra workstation. Typical times for the 3D filling cases were 1.3 CPU hours per 100 steps, 3000 timesteps were necessary to fill the mould, and each timestep required an average of 10 iterations to converge.

4 CONCLUSIONS

This paper demonstrates the successful use of a ray-tracing technique coupled to an explicit flux limiting scheme, to compute interface movement, fluid flow, solidification and heat transfer in a liquid metal/air system.

The validation results indicate that even for extremely complex meshes, the correct propagation speed is achieved, and smearing of the interface is prevented.

In order to fully describe the casting process, one needs to include the effects of macrosegregation, external radiation,

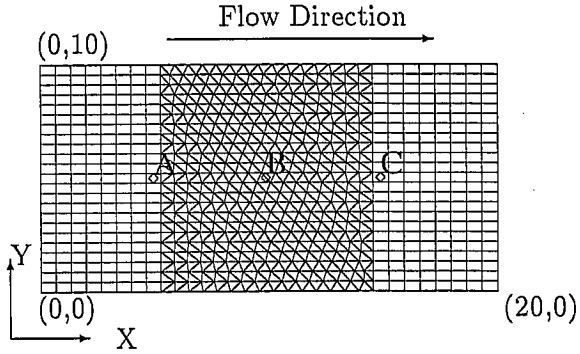

Figure 8: Mesh used for case 3.

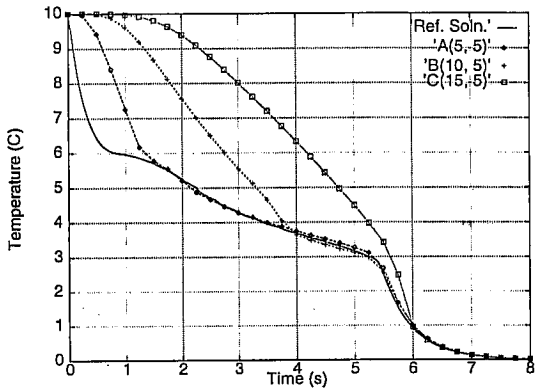

Figure 9: Temperature histories for validation case 3.

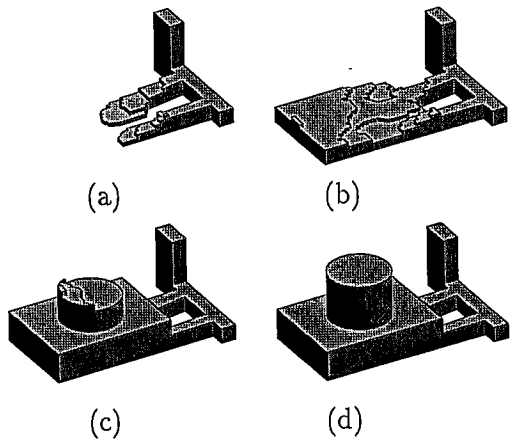

Figure 10: Time series of filling of a 3D cavity.

shrinkage and porosity. These effects can be modelled using much of the existing framework described in this paper. This work will be presented in the near future.

ACKNOWLEDGEMENTS

The financial assistance of the EPSRC is acknowledged in this work.

References

[1] K. S. Chan, K. A. Pericleous, and M. Cross, 1991, " Numerical simulation of flows encountered during mould filling." Appl. Math. Modelling. **15**, pp 624-631.

[2] K. A. Pericleous, K. S. Chan, and M. Cross, 1995, "Free surface flow and heat transfer in Cavities: the SEA algorithm.", Numerical Heat Transfer, Part B, **27**, pp 487.

[3] J. Campbell, *Castings*, (Butterworth-Heinemann, Oxford, 1991).

[4] Liu Jun and D. B. Spalding, 1988, " Numerical simulations of flow with moving interface.", PCH Physico-Chemical Hydrodynamics, **10**, No. 5/6; pp 625-637.

[5] B. van Leer, 1977, "Towards the Ultimate Conservation Difference Scheme. IV A New Approach to Numerical Convection." J. Comp. Phys., **23**, pp 276.

[6] C. W. Hirt and B. D. Nichols, 1981, " Volume of Fluid (VoF) method for the dynamics of free boundaries.", J. Comp. Phy., **39**, pp 201.

[7] M. Cross and J. Campbell (eds), 1995,"Modeling of Casting, Welding and Advanced Solidification Processes VII", published by the Materials, Metals and Minerals Society, Warrendale, PA.

[8] C. Bailey, P. Chow, M. Cross, Y. Fryer and K. Pericleous, 1996, " Multiphysics modelling of the metals casting process.", Proc. R. Soc. Lond. A, **452**, pp 459-486.

[9] PHYSICA, University of Greenwich, London, UK. Email physica@gre.ac.uk

[10] D. B. Spalding, 1974, "A Method for Computing Steady and Unsteady Flows Possessing Discontinuities of Density.", CHAM Report 910/2.

[11] P. Chow, K. A. Pericleous and M. Cross, 1995, "Numerical modelling of free surface flows in the metal castings process with finite volume unstructured mesh techniques.", Numerical methods in Laminar and Turbulent Flow (Eds C. Taylor, P. Durbetaki), **9**, Part II, pp 1076–1087.

[12] B. P. Leonard, 1988, "Universal Limiter for Transient Interpolation Modelling of the Advective Transport Equations", Tech. Memo 100916, NASA Lewis, Cleveland, OH.

[13] S. V. Patankar and D. B. Spalding, 1972, "A Calculation Procedure for Heat, Mass and Momentum Transfer in Three-Dimensional Parabolic Flows", Int. J. Heat Mass Transfer, **15**, pp 1787.

[14] C. M. Rhie and W. L. Chow, 1982, "A numerical study of the turbulent flow past an isolated aerofoil with trailing edge separation", AIAA July, **21**, pp 1525-1532.

[15] J. C. Martin and W. J. Moyce, 1952, "An experimental study of the collapse of liquid column on a rigid horizontal plane.", Phil. Trans. R. Soc. **244**, pp 312.